Side Slip Angle Based Control Threshold of Vehicle Stability Control System

Taeyoung Chung
PhD Candidate, Automotive Engineering, Hanyang University, 17 Haengdang-dong, Seongdong-gu, Seoul 133-791, Korea
Kyongsu Yi*
Professor, School of Mechanical Engineering, Hanyang University, 17 Haengdang-dong, Seongdong-gu, Seoul 133-791, Korea

Vehicle Stability Control (VSC) system prevents vehicle from spinning or drifting out mainly by braking intervention. Although a control threshold of conventional VSC is designed by vehicle characteristics and centered on average drivers, it can be a redundancy to expert drivers in critical driving conditions. In this study, a manual adaptation of VSC is investigated by changing the control threshold. A control threshold can be determined by phase plane analysis of side slip angle and angular velocity which is established with various vehicle speeds and steering angles. Since vehicle side slip angle is impossible to be obtained by commercially available sensors, a side slip angle is designed and evaluated with test results. By using the estimated value, phase plane analysis is applied to determine control threshold. To evaluate an effect of control threshold, we applied a 23-DOF vehicle nonlinear model with a vehicle planar motion model based sliding controller. Controller gains are tuned as the control threshold changed. A VSC with various control thresholds makes VSC more flexible with respect to individual driver characteristics.

Key Words: Vehicle Stability Control (VSC) System, Control Threshold, Side Slip Angle Estimator, Phase Plane Analysis

1. Introduction

A Vehicle Stability Control (VSC) system is an active safety system for road vehicles which stabilizes the vehicle dynamic behavior in emergency situations such as spinning, drift out, and roll over. When an excessive deviation between actual and driver intended lateral response is developing near a lateral stability margin, a VSC activated at the designed control threshold to stabilizes the vehicle. A conventional VSC is designed centered around the normal and average driver (Van Zanten, 1998). Most VSC installed vehicles have a switch which enables a driver choose the controller on and off. It is because an expert driver may feel redundancy by early VSC intervention, despite the stabilizing effort. About this discrepancy, Tseng discussed system transparency achieved by an actuation smoothness of VSC (Tseng et al., 1999). However a VSC adaptation of driver characteristics can be considered in control algorithm to satisfy any kind of drivers. It can be achieved by nominal value or control threshold adaptation. To obtain the nominal value of deferent kinds of driver relies heavily on field testing and is time-consuming and expensive. In this study, we investigate an effect of changing control threshold of VSC and propose

* Corresponding Author,
E-mail : kyongsu@hanyang.ac.kr
TEL : +82-2-2220-0455; **FAX** : +82-2-2296-0561
Professor, School of Mechanical Engineering, Hanyang University, 17 Haengdang-dong, Seongdong-gu, Seoul 133-791, Korea. (Manuscript **Received** November 25, 2004; **Revised** March 10, 2005)

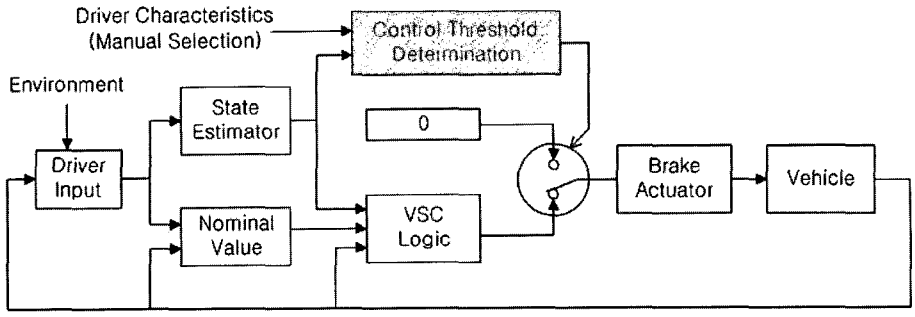

Fig. 1 VSC control scheme

a possibility of improving VSC by selecting the control threshold without changing nominal value. Fig. 1 is schematics of VSC algorithm proposed in this study.

To obtain more accurate vehicle stability limit, a vehicle side slip angle estimator which has robustness on disturbance is essential. If a performance of side slip angle estimator is acceptable, phase plane of a side slip angle and angular velocity can offer more practical information of vehicle stability limit (Inagaki et al.,1994 ; Nishio and Tozu, 2001). Vehicle state estimators for side-slip angle or lateral velocity are mainly classified into a kinematic, dynamic model based state observer, and Kalman filter (Kaminaga and Naito, 1998 ; Lee, 2003 ; Tseng, 2002), and a bank angle estimator increases their robustness (Tseng, 2000). The performances are evaluated under various test driving conditions.

With the state estimator, the VSC system with various control thresholds is evaluated using vehicle simulation model in a j-turn test. A vehicle simulation model consists of a vehicle body, suspensions, Pacejka tire models and powertrain models (Ha et al., 2003). A differential braking control law based on vehicle planar motions is used in the simulation (Yi et al., 2003).

2. Lateral Tire Model and Phase Plane Analysis

A vehicle lateral behavior is affected mainly by a lateral tire force characteristics. Eq. (1) shows a basic 2-D linear vehicle model which state variables are lateral velocity (v) and yaw rate (γ).

$$\dot{x}=Ax+B\delta \quad x=[v\ \gamma]^T$$
$$A=\begin{bmatrix} -\frac{C_f+C_r}{m\cdot u} & -u-\frac{aC_f-bC_r}{m\cdot u} \\ -\frac{aC_f-bC_r}{I_z} & -\frac{a^2C_f+b^2C_r}{I_z\cdot u} \end{bmatrix} \quad (1)$$
$$B=\begin{bmatrix} \frac{C_f}{m} & \frac{aC_f}{I_z} \end{bmatrix}^T$$

where, C_f, C_r are cornering power of front and rear wheel, m and I_z are vehicle mass and moment of inertia about yaw axis, u is vehicle longitudinal velocity, a and b are distances from center of gravity to front and rear axle. A lateral tire model is obtained by vehicle test with steady state cornering. With constant vehicle speed and step steering input, front and rear cornering powers, which indicate a relation between tire slip angle and lateral tire force, are calculated by a steady state value of 2-D linear vehicle model as follows.

$$\beta_{ss}=\frac{\{2b(a+b)C_fC_r-mu^2aC_f\}\delta}{2C_fC_r(a+b)^2-mu^2(aC_f-bC_r)}$$
$$\gamma_{ss}=\frac{2(a+b)C_fC_ru\delta}{2C_fC_r(a+b)^2-mu^2(aC_f-bC_r)} \quad (2)$$

where, β_{ss}, γ_{ss} are indicate steady state value of side slip angle ($\beta=v/u$) and yaw rate. Eq. (2) is rewritten as follows.

$$\{mu^2a(\delta-\beta_{ss})\}C_f+\{2\beta_{ss}(a+b)^2-2b(a+b)\delta\}C_fC_r$$
$$+\{\beta_{ss}mu^2b\}C_r=0$$
$$\{mu^2a\gamma_{ss}\}C_f+\{2\gamma_{ss}(a+b)^2-2(a+b)u\delta\}C_fC_r \quad (3)$$
$$+\{\gamma_{ss}mu^2b\}C_r=0$$

By solving Eq. (3), front and rear cornering power is obtained with respect to vehicle test data

of each constant steering angle. Fig. 2 shows that the test results of vehicle speed at 100 kph and modified magic formula tire model. The side slip angle is measured using an optical sensor. Shape, stiffness and magnitude factors of tire model are modified to fit the test results.

A phase plane of vehicle side slip angle and angular velocity is obtained by with 2-D vehicle model in various initial conditions. 2-D vehicle model with magic formula tire model is as follows.

$$\begin{aligned} mu(\dot{\beta}+\gamma) &= F_{yf}+F_{yr} \\ I_z\dot{\gamma} &= aF_{yf}-bF_{yr} \end{aligned} \tag{4}$$

where, F_{yf} and F_{yr} are front and rear lateral tire force obtained by magic formula which is represented in Fig. 2. A phase plane of 100 kph and 100 deg steering wheel angle (SWA) is shown in the Fig. 3. A physical vehicle stability limit can be simply determined by saddle point of side slip angle and the inclinations as c_i in the figure.

In the driving condition, control threshold of VSC is assumed as combinations of each c_i and control threshold factor f_{ct} $(0<f_{ct}\leq 1)$ shown in the figure. The ideal vehicle stability limits of each driving condition are needed to be obtained as look-up table for a practical application.

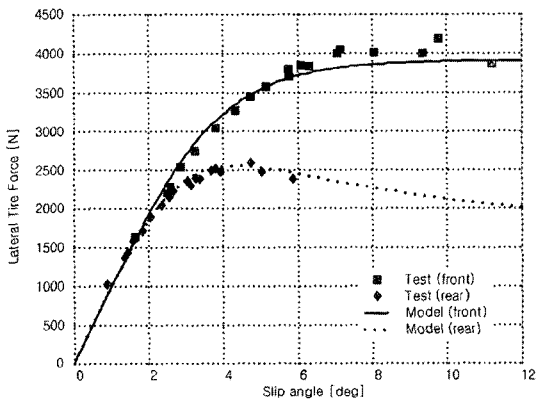

Fig. 2 Lateral tire force characteristics

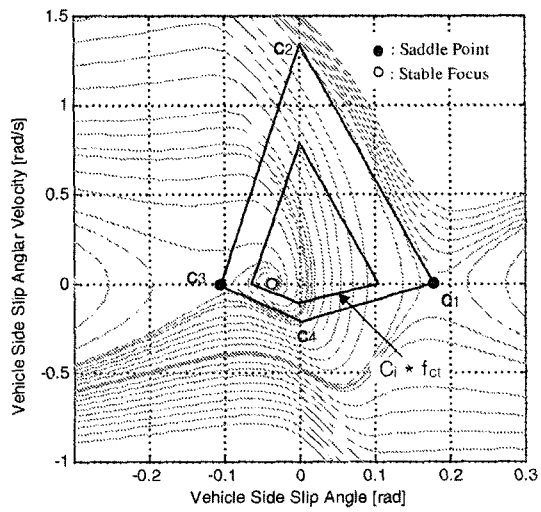

Fig. 3 $\beta-\dot{\beta}$ phase plane (100 kph 100 SWA)

3. Control Threshold and Controller Parameters

When a negative step steering input is applied, a trajectory of vehicle behavior in phase plane is going to positive limit value as shown in Fig. 4. A VSC is activated when the trajectory met designed control threshold which represents average driver. It is also less than ideal vehicle stability limit with designed margin due to a delay of actuator dynamics and characteristics of average driver. If the trajectory approaches toward control threshold, VSC checks that the difference is within some tolerable dead zone, if not, it generates a yaw moment to stabilize the vehicle. If the designed VSC threshold represents an average driver, a recognized stability limit of an expert driver could be higher than VSC threshold, and

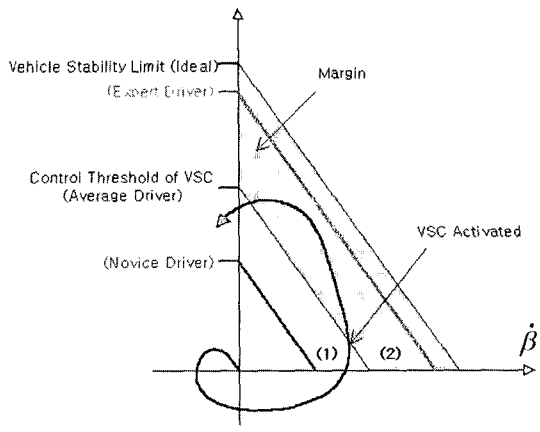

Fig. 4 Ideal vehicle stability limit and VSC control threshold

that of a novice driver could be lower. Thus, in the region (1) in the figure, VSC is not activated, and a novice driver could feel dangerous. In the region (2), VSC is activated, and an expert driver could feel redundancy. Whether it is determined or tuned by a researcher or a test driver, the control threshold cannot satisfy all drivers. If a driver can select the VSC threshold, a VSC system has flexibility with respect to driver characteristics.

Since lateral and longitudinal motions of a vehicle are governed by longitudinal and lateral tire forces and the tire forces can be controlled by driving shaft torque and brake forces, the controller is designed using a three-degree of freedom vehicle planar motion model with inputs of brake pressures of the wheels. The desired value of the yaw rate is computed based on the driver's steering input and vehicle longitudinal speed using a linear tire model as follows (Tseng et al., 1999).

$$r_{des}=\frac{u}{(a+b)\,(1+u^2/u_{ch}^2)}\delta \tag{5}$$

where, u_{ch} is characteristic velocity of the vehicle. Since the lateral acceleration is limited by the friction coefficient between the tires and the road, the desired yaw rate is also limited under the value, $\mu g/u$. Sliding controllers are designed to minimize the side slip angle and a weighted combination of yaw rate error and side slip angle presented by Uematsu and Gerdes (Uematsu and Gerdes, 2002).

$$s=r_{des}-r+\rho\cdot\beta \tag{6}$$

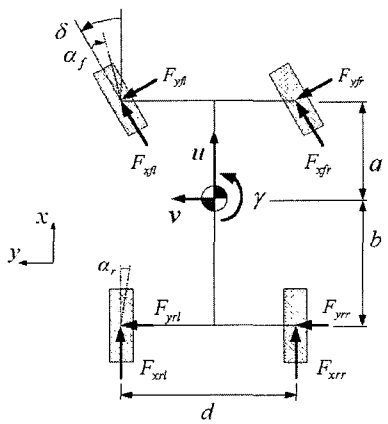

Fig. 5 Vehicle planar motion model

where, the scalar, s, is a combination of sideslip angle, γ_{des}, and the difference between the desired yaw rate and actual yaw rate. ρ is a positive constant. The controller derived from (6) achieves the basic objectives and parametric robustness of VSC and robustness more successfully than a controller built on either side slip angle or yaw rate alone.

Equations of motions describing vehicle yaw plane model are as follows:

$$\begin{aligned} m\dot{v}&=F_{yr}+F_{xf}\sin\delta+F_{yf}\cos\delta-mru\\ I_z\dot{r}&=aF_{xf}\sin\delta+aF_{yf}\cos\delta-bF_{yr}\\ &\quad+\frac{d}{2}(F_{xfr}-F_{xfl})\cos\delta+\frac{d}{2}(F_{xrr}-F_{xrl}) \end{aligned} \tag{7}$$

where, d is track width, F_x is traction force. By simplifying lateral and longitudinal tire force, sliding control law of Eq. (8) is applied to calculate control inputs.

$$\dot{s}=-K\cdot s \tag{8}$$

Control inputs of front wheels are derived form Eqs (5) ~ (8) as follows.

$$P_{Bfl,command}=\begin{cases}\dfrac{N_{l,nb}}{D_{l,nb}}f_{ca} & \text{if } \dfrac{N_{l,nb}}{D_{l,nb}}\geq 0\\ 0 & \text{if } \dfrac{N_{l,nb}}{D_{l,nb}}<0\end{cases}$$

$$P_{Bfr,command}=\begin{cases}\dfrac{N_{r,nb}}{D_{r,nb}}f_{ca} & \text{if } \dfrac{N_{r,nb}}{D_{r,nb}}\geq 0\\ 0 & \text{if } \dfrac{N_{r,nb}}{D_{r,nb}}<0\end{cases} \tag{9}$$

where, N and D are numerator and denominators derived from Eq. (8), $P_{Bf,command}$ is front brake pressure control input. A control flag, f_{ca} is 1, when the control threshold determination logic determines to activate the controller, or f_{ca} is 0. Controller parameters, sliding gain K and weighting factor of side slip angle ρ have to be changed as variations of control threshold.

A control flag is determined by following procedure as Fig. 6. To prevent measurement noise, a sensitivity gap of $\dot{\beta}$ is considered. Second, the algorithm checks if the trajectory deviates from designed control threshold. Third, gradients have to be checked whether the trajectory toward stable region or not.

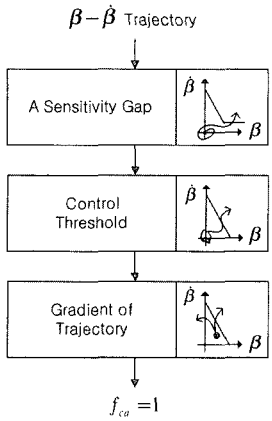

Fig. 6 Control flag determination algorithm

4. Side Slip Angle Estimator

A linear model based observer for lateral velocity estimation is affected by nonlinearity of lateral tire force. To overcome the weakness, a cornering power estimator based adaptive observer is presented. The key design parameter is weighting matrix of Lyapunov function, and it is hard to find the parameter which satisfies all kinds of driving situation. A kinematic model based discrete-time Kalman filter using approximated longitudinal and lateral velocity is also presented in this study. Finding noise covariance of each estimate is important to design this estimator. Eq. (10) shows that kinematic model based discrete-time state equation.

$$x_{k+1}=A_k x_k+Bu_k+B_q q \quad y_k=Cx_k+r$$
$$x_k=\begin{bmatrix}u_k\\ v_k\end{bmatrix} u_k=\begin{bmatrix}a_{xk}\\ a_{yk}\end{bmatrix} A_k=\begin{bmatrix}1 & T\gamma_k\\ -T\gamma_k & 1\end{bmatrix} \tag{10}$$
$$B=\begin{bmatrix}T & 0\\ 0 & T\end{bmatrix} B_q=\begin{bmatrix}T & 0\\ 0 & T\end{bmatrix} y_k=\begin{bmatrix}u_{ak}\\ v_{ak}\end{bmatrix} C=\begin{bmatrix}1 & 0\\ 0 & 1\end{bmatrix}$$

where, k represents iteration step, T is sampling time, a_x and a_y are longitudinal and lateral accelerations, u_a and v_a are approximated measurement of longitudinal and lateral vehicle velocity which is obtained by linear state observer with constant gain K_{obs}. A linear state observer equation is as follows

$$\dot{\hat{x}}=A\hat{x}+Bu+K_{obs}(y-C\hat{x}-Du) \tag{11}$$

where, measurement y is yaw rate. Fig. 7 shows

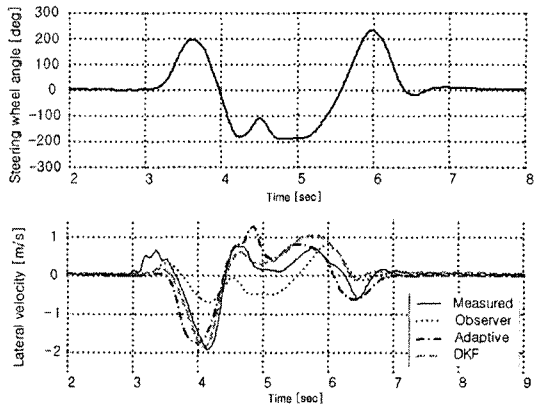

Fig. 7 Lateral velocity estimation results (severe lane change)

that the test results of 80 kph severe lane change. The driver starts lane change at 3 second, finishes at 4.5 second, and stabilizes through end of the maneuver.

Although large slip angle is caused in the severe lane change, adaptive observer and Kalman filter estimates are similar as test data at the first large lateral velocity region about 4 second, while linear state observer result shows poor performance. After the lane change, adaptive observer estimate shows a transient error around 5 second. This transient can be the point whether VSC activated or not; the Kalman filter is said to be better performance of that point. In this study, we applied discrete-time Kalman filter for further studies. Fig. 8 shows that the test results of 100 kph 100 SWA j-turn test.

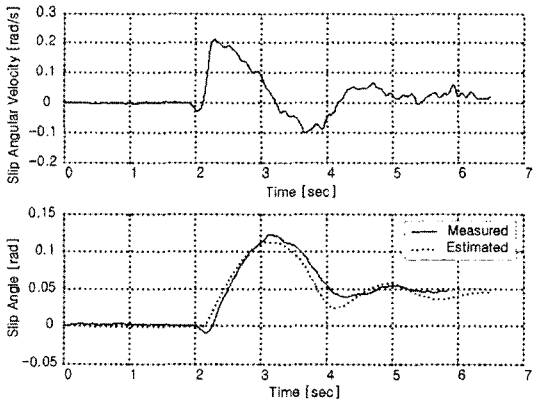

Fig. 8 Lateral velocity estimation results (j-turn)

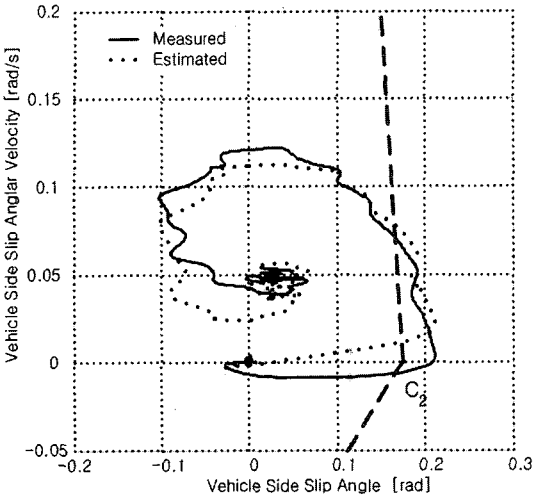

Fig. 9 Comparison of measured and estimated trajectories on phase plane (j-turn)

The asterisks on the trajectories indicate that the step steering maneuver finished and maintained 100 degree. Although estimated trace is bigger than the measured one around the stability limit, its tendency is similar. This difference should be handled by changing control threshold.

5. Simulation Results

A controller parameter is determined as control threshold variations using 23-DOF nonlinear vehicle simulations. Sensor resolutions and noise characteristics are considered similar as test results, and actuator dynamics is considered as brake pressure increasing rate of 75[bar/s]. An open-loop maneuver of fish-hook test is shown in the Fig. 10.

Figure 11 shows the simulation results in the case of f_{ct} is 0.3, an early intervention of VSC. The dashed line indicates a trajectory of uncontrolled case, and a solid line indicates controlled case. Brake torque of each wheel is shown below in the figure. In this case, brake torque is applied region (1) to (2), and (2) to (3), and transient response at region (3) near 600 N. The control parameters, K and ρ, are chosen for smoother vehicle responses. Fig. 12 shows the simulation

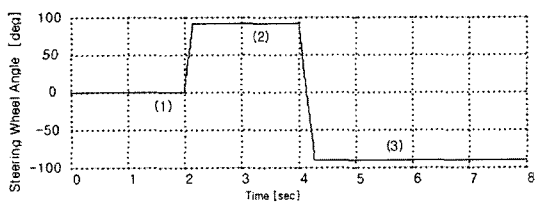

Fig. 10 Steering wheel angle of fish-hook test

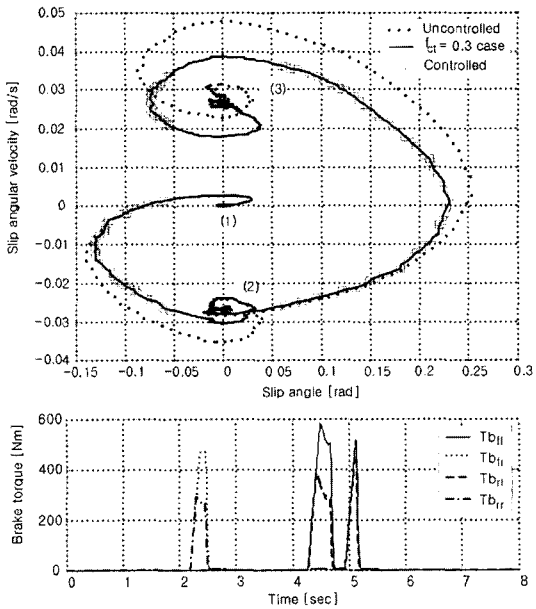

Fig. 11 Fish-hook simulation results (f_{ct}=0.3 case)

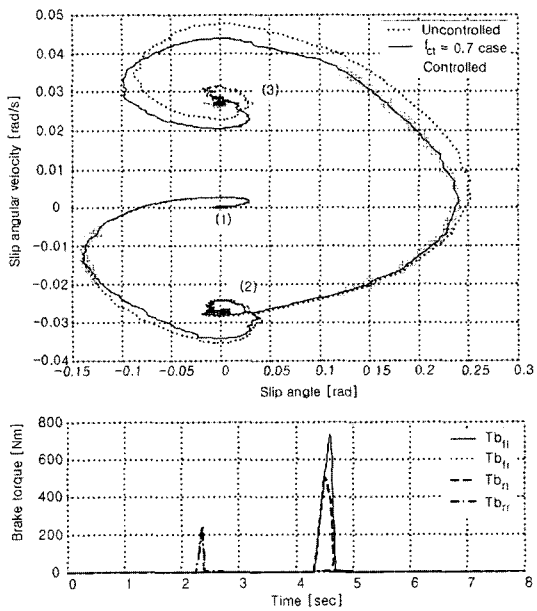

Fig. 12 Fish-hook simulation results (f_{ct}=0.7 case)

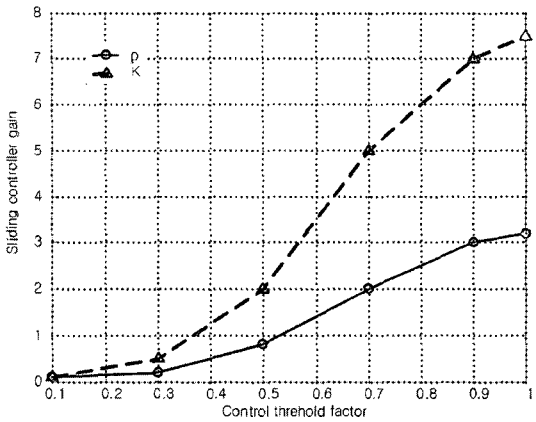

Fig. 13 Control threshold factors and controller parameters

results in the case of f_{ct} is 0.7, a late intervention case. In this case, brake torque is applied less than the previous case. Relatively fast control intervention is needed in this late intervention case, thus control parameters have to be bigger than the previous case. Fig. 13 shows that the relationship with control threshold factor and sliding controller parameters. When f_{ct} is relatively small, an early intervention of control input is applied. To make a driver feel comfortable, brake inputs have to be small. If f_{ct} is near 1, late intervention case, controller input has to stabilize the vehicle in relatively short time, and brake input have to be large.

6. Conclusions

A VSC improvement by means of changing its control threshold in the control algorithm is investigated. To determine control threshold, phase plane analysis is used. A side slip angle estimator is evaluated using test data for determine trajectory in phase plane. Vehicle planar motion model based sliding controller, which sliding surface is defined as weighted combinations of yaw rate error and side slip angle, is applied in vehicle nonlinear simulations. Controller parameters are determined using fish-hook test with various control threshold factor. As shown in the figure below, a driver can select the VSC property by variable switch rather than on/off switch.

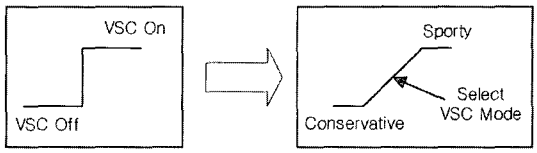

Fig. 14 VSC improvement with control threshold

For future work, a driving simulator based human-in-the-loop evaluations (Chung et al., 2004) have to be conducted for simulation study in the laboratory. An adaptive VSC would be feasible by adapting the control threshold based on human driver characteristics.

Acknowledgments

This research is supported by National Research Laboratory (NRL) project.

References

Chung, T., Kim, J. and Yi, K., 2004, "Human-in-the-Loop Evaluation of a Vehicle Stability Controller Using a Vehicle Simulator," *International Journal of Automotive Technology*, Vol. 5, No. 2, pp. 109~114.

Ha, J., Chung, T., Kim, J., Yi, K. and Lee, J., 2003, "Validation of 3D Vehicle Model and Driver Steering Model with Vehicle Test," *Spring Conference Proceeding of KSAE*, Vol. 2, pp. 676~681.

Inagaki, S., Kshiro. I. and Yamamoto, M., 1994, "Analysis on Vehicle Stability in Critical Cornering," *Proceedings of the Int. Symposium on Advanced Vehicle Control*, 9438411, pp. 287~292.

Kaminaga, M. and Naito, G., 1998, "Vehicle Body Slip Angle Estimation Using an Adaptive Observer," *Proceedings of the Int. Symposium on Advanced Vehicle Control*, 9836635, pp. 207~212.

Lee, H., 2003, "Reliability Indexed Sensor Fusion and Its Application to Vehicle Longitudinal and Lateral Velocity Estimation," *International Journal of Vehicle Design*, Vol. 33, No. 4, pp. 351~364.

Nishio, A. and Tozu, K., 2001, "Development

of Vehicle Stability Control System Based on Vehicle Sideslip Angle Estimation," SAE Transactions, 2001-01-0137.

Tseng, H. E., Ashrafi, B., Madau, D., Brown, T. A. and Recker, D., 1999, "The Development of Vehicle Stability Control at Ford," *IEEE/ASME Transactions on Mechatronics*, Vol. 4, No. 3, pp. 223~234.

Tseng, H., 2002, "A Sliding Mode Lateral Velocity Observer," *Proceedings of the Int. Symposium on Advanced Vehicle Control*, 20024542, pp. 387~392.

Tseng, H., 2000, "Dynamic Estimation of Road Bank Angle," *Proceedings of the Int. Symposium on Advanced Vehicle Control*, pp. 421~428.

Uematsu, K. and Gerdes, J. C., 2002, "A Comparison of Several Sliding Surfaces for Stability Control," *Proceedings of the Int. Symposium on Advanced Vehicle Control, Hiroshima*, Japan.

Van Zanten, A. T., 1998, "Evolution of Electronic Control Systems for Improving the Vehicle Dynamic Behavior," *Proceedings of the Int. Symposium on Advanced Vehicle Control*, 20024481, pp. 7~15.

Yi, K., Chung, T., Kim, J. and Yi, S., 2003, "An Investigation into Differential Braking Strategies for Vehicle Stability Control," *IMechE*, Vol. 217, Part D, pp. 1081~1093.